THE JOURNAL OF PHYSICAL CHEMISTRY B

Article

pubs.acs.org/JPCB

A Systematic Approach for Development of an OPLS-Like Force Field and Its Application to Hydrofluorocarbons

E. Paulechka,[†,‡,§] K. Kroenlein,[*,†] A. Kazakov,[†] and M. Frenkel[†]

[†]Thermophysical Properties Division, National Institute of Standards and Technology, Boulder, Colorado 80305-3337, United States

[‡]Chemistry Department, Belarusian State University, Minsk 220030, Republic of Belarus

Supporting Information

ABSTRACT: A systematic, formal approach to optimization of force field parameters for molecular simulations is presented. The procedure is based on response surface mapping methodology that allows simultaneous parameter optimization against multiple property targets while constraining the number of required computationally expensive numerical experiments. The approach was implemented for prediction of vapor−liquid equilibrium properties of alkanes, alkenes, and their fluorinated derivatives via Monte Carlo molecular simulations. To further reduce computational costs, a bootstrap procedure that involves a sequence of parameter optimization for four pairs of compounds (ethane and propane, ethene and propene, perfluoroethane and perfluoropropane, and 2,3,3,3-tetrafluoropropene and (*E*)-1,3,3,3-tetrafluoropropene) was used. The results of simulations utilizing the optimized force field parameters agree well with associated reference equations of state.

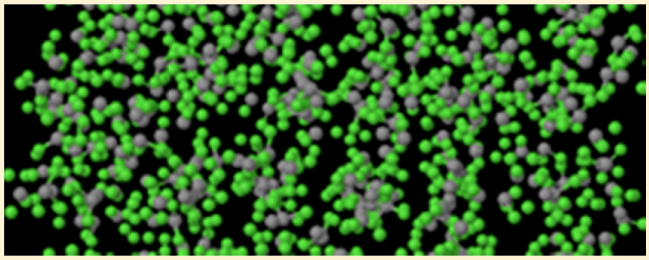

INTRODUCTION

Molecular simulation methods including Monte Carlo (MC) and molecular dynamics are gradually emerging as powerful tools for quantitative description of thermodynamic properties.[1] Modern computational resources allow MC simulations of vapor−liquid equilibrium (VLE) for systems containing hundreds of molecules or ions. A typical VLE simulation for a system of small polyatomic molecules requires hundreds to thousands of hours on a single computational core with present hardware; in some cases this time reaches ~3 × 10^4 h.[2] Modeling the entire VLE curve via a series of simulations spanning the associated temperature range increases this time by an order of magnitude. Taking into account rapid advances in computer hardware as well as in the numerical algorithms, one may anticipate that performing hundreds of individual molecular simulations in a reasonable time will be possible in the near future.

The issue of critical importance for quantitative predictions is the availability of a well-calibrated force field. Determination of force field parameters requires significant computational resources and substantial human expertise. To accommodate the anticipated need in large-scale modeling, it would be desirable to have formal procedures for force field development which would promote automation of the process and decrease the degree of expert involvement. In this work, we propose a systematic methodology for determination of force field parameters and apply these force fields to simulation of VLE in alkanes, alkenes, and their fluoroderivatives.

Alkanes and alkenes are normally used for calibration and validation of new experimental or computational procedures. Fluoroalkanes are required to get force field parameters for fluoroalkenes. Two fluoroalkenes have received increased attention recently: 2,3,3,3-tetrafluoropropene (HFO-1234yf) is considered as a promising material for replacement of current refrigerants[3] and (*E*)-1,3,3,3-tetrafluoropropene (HFO-1234ze-(E)) is already used as a blowing agent in aerosols and foams.[4] Low environmental impact, low toxicity and flammability, and plastics compatibility are among the advantages of these materials. A number of experimental studies on thermophysical and thermodynamic properties for HFO-1234yf and HFO-1234ze(E) have been reported.[5−23] Several force field parametrizations have been proposed for alkane, alkene, and fluoroalkane systems.[24−29] All these force fields are generally developed by heuristic means, though some formal procedures for force field optimization have been considered.[30,31]

More recently, force field for simulation of VLE for fluoropropenes has been proposed.[32−35] In the force field by Raabe and Maginn,[32,34,35] most intramolecular parameters and atomic charges were obtained from quantum-chemical calculations. The Lennard-Jones parameters were derived using the experimental liquid density and vapor pressure data for 2,3,3,3-tetrafluoropropene and 3,3,3-trifluoropropene, as well as the density and enthalpy of vaporization for tetrafluoroethene. The temperature range, as well as the details of the procedure used for optimization of parameters, was not completely specified. In our previous work,[33] a force field

Received: September 13, 2012
Revised: November 16, 2012

derived from the original OPLS-AA[36] was used. New parameters for the fluorine atom attached to a double-bonded carbon atom were introduced. The Lennard-Jones parameters and atomic charge for this atom were obtained by matching the liquid density of HFO-1234yf at the normal boiling point via a series of numerical experiments arranged in a 2^3 factorial design.

THEORETICAL METHODS

Calculations. MC simulations were carried out with the MCCCS TOWHEE v. 6.2.6 package,[37] modified in-house to include a more recent pseudorandom number generator (RNG) from Brent.[38] The Brent RNG is capable of generating the necessary stream of numerical output at a substantially lower computational overhead than the default RNG for the simulation package RANLUX, level 3 RNG.[39] Both algorithms are known to pass robust tests for statistical distribution of the generated output, while usage of the more recent algorithm resulted in a speed-up of better than 30% for the entire simulation, as measured by wall time.

The energy of the system was calculated using the OPLS-AA force field according to the equation

$$U = \sum_{\text{bonds}} k_r(r - r_0)^2 + \sum_{\text{angles}} k_\theta(\theta - \theta_0)^2 + \sum_{\text{dihedrals}} \sum_{l=1}^{3} k_l(1 - (-1)^l \cos l\varphi) + \sum_i \sum_j f_{ij}\left(4\varepsilon_{ij}\left(\left(\frac{\sigma_{ij}}{r_{ij}}\right)^{12} - \left(\frac{\sigma_{ij}}{r_{ij}}\right)^{6}\right) + \frac{1}{4\pi\varepsilon_0}\frac{q_i q_j}{r_{ij}}\right) \quad (1)$$

where k_r, k_θ, and k_l are force constants, ε and σ are Lennard-Jones well depths and diameters, q is the Coulombic charge, and f_{ij} is the OPLS-AA "fudge factor" of 0.5 for atoms 3 or more bonds apart; 1.0 otherwise. The parameters for stretching, bending, and torsions were taken from the original OPLS-AA force field.[36] The parameters for C═C—C—F torsion reported in our previous paper[33] were used here as well. The Lennard-Jones parameters for pairs of different atoms were obtained from the geometric-mean combining rules as postulated in OPLS-AA. A complete list of parameters used in the calculations is presented in Tables A1-A12 in the Supporting Information.

In the original OPLS-AA, force field atomic charges are assigned empirically. We used these assignments previously,[33] but the calculated vapor pressures for HFO-1234yf were too high as compared with the experimental data. In this work, atomic charges were calculated according to the CHELPG scheme[40] at the HF/6-31+G(d) theory level using Gaussian 03.[41] Initially, we also tested the usage of Mulliken atomic charges;[42] it was found that they cannot provide a satisfactory description of the experimental VLE data for fluoropropenes, although for the other compounds a reasonable agreement can be achieved. Partial charges were determined for a minimum-energy optimized geometry.

The vapor−liquid simulations were performed in the Gibbs two-box ensemble.[43−45] Initially, each box contained 216 molecules, thus yielding a total of 432 molecules. A nonbond cutoff of 1 nm with analytical tail corrections[46] was applied for the Lennard-Jones interactions. Electrostatic interactions were treated using the Ewald sum technique[47] with a constant number of inverse space vectors. The following move probabilities were adopted: 0.33 for translation and rotation, 0.32 for configurational-bias regrowth,[48] 0.01 for aggregation-volume bias in the AVBMC2 implementation,[49] 0.008 for interbox swap, and 0.002 for box volume change. The maximum displacements for translation, rotation, and box volume change were periodically adjusted to yield the acceptance rate of 50%.

Simulations used for optimization of force field parameters included 40 000 MC equilibration cycles followed by 20 000 MC production cycles. Simulations used for the final calculations of VLE-related properties included 70 000−80 000 MC equilibration cycles followed by 40 000 MC production cycles. A cycle was defined as a number of MC moves equal to the number of molecules in the system. The average values of density, enthalpy of vaporization and saturated vapor pressure were recorded for each set of 8000 MC cycles. The statistical uncertainties of these properties, defined as their standard deviations, were determined based on these data.

The saturated vapor pressures, p_{sat}, were calculated from the molecular virial for the gas box. The molar enthalpies of vaporization, $\Delta_{vap}H_m$, were calculated from the equation

$$\Delta_{vap}H_m = U_{g,m} - U_{l,m} + p_{sat}M\left(\frac{1}{\rho_g} - \frac{1}{\rho_l}\right) \quad (2)$$

where $U_{g,m}$ and $U_{l,m}$ are the calculated molar energies of the gas and liquid phases, ρ_g and ρ_l are their mass densities, and M is the molar mass of a compound.

The critical temperature, T_c, and the critical density, ρ_c, were determined by simultaneously fitting ρ_l and ρ_g with the following equations

$$\rho_l - \rho_g = B(T_c - T)^\beta \quad (3)$$

$$\frac{(\rho_l + \rho_g)}{2} = \rho_c + A(T_c - T) \quad (4)$$

where A and B are the fitted parameters, T is the temperature, and $\beta = 0.32$ is the Ising-type critical exponent. The temperature dependence of p_{sat} was described by the equation

$$\ln p_{sat} = C - D/T \quad (5)$$

whose parameters C and D were determined by the calculated p_{sat} values at different temperatures. The critical pressure, p_c, was calculated by substitution of the previously obtained T_c into eq 5. In the fitting procedures, uncertainties of the calculated values were considered.

The reported uncertainties in the calculated critical parameters as well as in all the experimental data correspond to 95% confidence intervals (coverage factor $k = 2$). Reported uncertainties for calculated critical parameters are representative of statistical variation within simulations and do not represent a measure of prediction reliability.

Force Field Development. The primary goal of the present work is a force field capable of predicting the VLE properties of hydrofluorocarbons. This introduces two important points into defining the procedure for determination of force field parameters. First, VLE properties are relatively insensitive to the intramolecular parameters describing stretching, bending, and torsion, and only the Lennard-Jones

dx.doi.org/10.1021/jp309119h | J. Phys. Chem. B XXXX, XXX, XXX−XXX

parameters and atomic charges affect the properties of interest. Atomic charges, in turn, can be derived from quantum chemical calculations. Therefore, only the Lennard-Jones parameters were optimized.

Since the VLE properties are of interest, optimization of parameters should be carried out using available experimentally derived recommended data for saturated vapor pressure, enthalpy of vaporization, and liquid density. Deviations of gas density from the ideal-gas approximation become significant only well above the normal boiling temperature, and thus vapor density was not used for force field optimization.

The compounds of interest included C2 and C3 alkanes, alkenes, and their fluoro-derivatives. The following atomic types were introduced: CT and HC-1 types for C and H atoms of alkanes, CM and HC-2 types for)C= atom and H atom next to a double bond, CTf and Fpf for atoms of CF_3- group, and CMf and Fcm types for a double-bonded C and attached F atom. Each atomic type has two Lennard-Jones parameters, including a potential well depth and diameter, with the total number of optimized parameters equal to 16.

Parameter optimization was performed by use of a solution mapping methodology.[50−52] To obtain the response surfaces for various properties, numerical experiments arranged in a circumscribed central composite design (CCD) scheme[53] were performed. If a compound has n unknown parameters, the total number of numerical experiments at one temperature needed to fill the design matrix is $(n + 1)^2$. C2 and C3 compounds used for determination of parameter values (Table 3) have 4, 8, or 12 unknown parameters that correspond to 25, 81, or 169 runs. To adequately reproduce the temperature dependence of the properties and to provide extrapolation of the VLE curve to the critical point, simulations for each compound were performed at least at four temperatures. Therefore, direct application of CCD for solution mapping would require an impractical amount of computational effort.

In order to decrease the computational time, the following bootstrap procedure was adopted (Figure 1). First, simulations are performed at four temperatures for a compound that has four adjustable parameters according to a CCD scheme. Using the resultant data, preliminary optimization of these parameters is carried out. The preliminary values of the parameters are used to tune the boundaries of the CCD scheme for calculations on the second compound with the same parameters. Then, based on the results for both compounds, optimized parameters are obtained. These optimized parameters are then utilized for the simulation of molecules which contain as-yet unoptimized parameter sets. Sets of co-optimized compounds are specified in Figure 1 with red outlines. In this way, rather than being subject to the n^2 scaling associated with simultaneous optimization of all parameters required for hydrofluoroolefin simulation, total required optimization steps were reduced to a linear scaling in compound number and in parameter count.

The described procedure was subsequently applied to all groups of the optimized parameters, which took 800 MC runs in total. The temperatures of simulation were selected to be $T_{b,eos}$, $0.73T_{c,eos}$, $0.80T_{c,eos}$, and $0.87T_{c,eos}$, where T_b is the temperature of the boiling point at 100 kPa, and the subscript "eos" implies the result obtained from an experimentally derived reference equation of state.[54]

To find the response functions, the variables were normalized and varied from $-\alpha$ to α in various points of the CCD plan, where $\alpha = 2$ for a four-variable design.[53] For density and

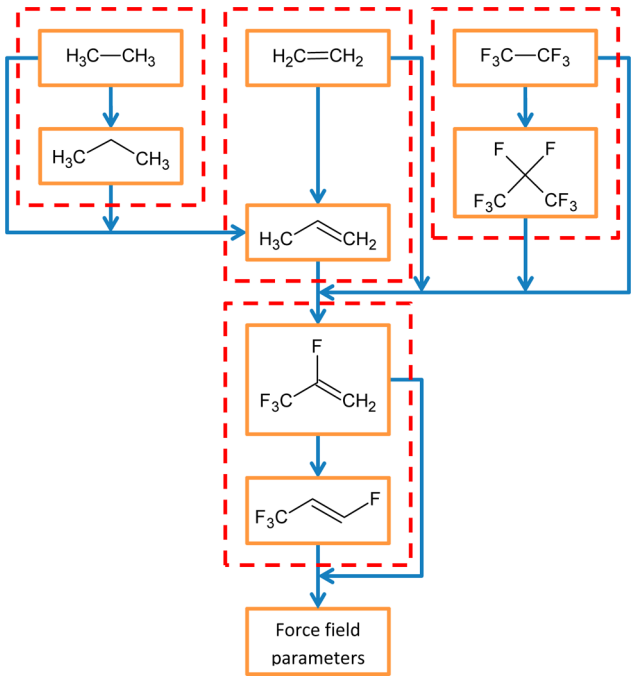

Figure 1. A scheme of a bootstrap procedure used for optimization of force field parameters.

enthalpy of vaporization, the response functions were polynomials describing relative deviations of these properties from the value in the central point of the plan. For p_{sat}, the response function described deviations of ln p_{sat} from that in the central point of the plan. Linear x_i and quadratic x_i^2 terms for every optimized parameter as well as cross terms x_ix_j were allowed in these functions.

The objective function used for determination of the Lennard-Jones parameters had the form

$$F = \sum [\ln(p_{calc,i}/p_{eos,i})]^2 + \sum \left(\frac{\Delta_{vap}H_{calc,i} - \Delta_{vap}H_{eos,i}}{\Delta_{vap}H_{eos,i}} \right)^2 + \sum \left(\frac{\rho_{calc,i} - \rho_{eos,i}}{\rho_{eos,i}} \right)^2 \quad (6)$$

Equation 6 accounts for all three properties with equal statistical weights.

The selection of target compounds (Table 3) was based on two criteria. First, for the bootstrapping procedure to work, it is necessary to make optimization of different parameters as independent as possible. The second criterion is availability of reliable VLE data from multiple sources. All compounds used have reference equations of state developed by fitting all available data for the properties within the scope[11,55−60] (as implemented in REFPROP[54]). Unlike prior efforts,[32] we did not use tetrafluoroethene and 3,3,3-trifluoropropene for optimization of force field parameters. At the time of this writing, only two sources[61,62] reporting liquid density and saturated vapor pressure for tetrafluoroethene were available, and the latter work[62] provides only equations describing the temperature dependence of properties. The liquid density of 3,3,3-trifluoropropene was reported in only one source[63] at

dx.doi.org/10.1021/jp309119h | J. Phys. Chem. B XXXX, XXX, XXX−XXX

temperatures much higher than the normal boiling temperature.

RESULTS AND DISCUSSION

Analysis of Response Functions. For each class of compounds, the influence of parameters for a pair of the inner

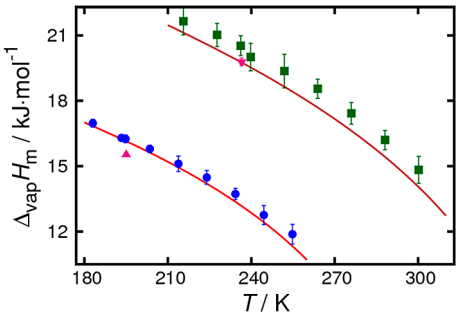

Figure 2. Enthalpies of vaporization of fluoroalkanes: (●) C_2F_6 simulation, (▲) C_2F_6 results of Watkins and Jorgensen,[28] (red line) C_2F_6 Lemmon and Span EOS,[59] (■) C_3F_8 simulation, (▼) C_3F_8 results of Watkins and Jorgensen,[28] and (purple line) C_3F_8 Lemmon and Span EOS.[59]

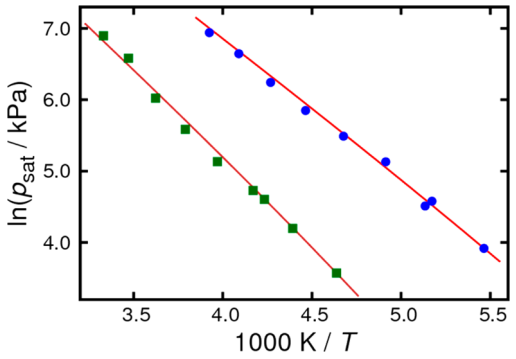

Figure 3. Saturated vapor pressure of fluoroalkanes: (●) C_2F_6 simulation, (red line) C_2F_6 Lemmon and Span EOS,[59] (■) C_3F_8 simulation, and (purple line) C_3F_8 Lemmon and Span EOS.[59] Estimated uncertainties on simulation are too small to be visible on this scale.

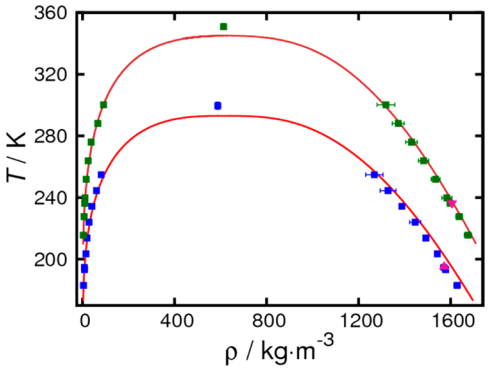

Figure 4. Saturated densities of fluoroalkanes: (●) C_2F_6 simulation, (▲) C_2F_6 results of Watkins and Jorgensen,[28] (red line) C_2F_6 Lemmon and Span EOS,[59] (■) C_3F_8 simulation, (▼) C_3F_8 results of Watkins and Jorgensen,[28] and (purple line) C_3F_8 Lemmon and Span EOS.[59]

C atom (σ_{in} and ε_{in}) and the outer H or F atom (σ_{out} and ε_{out}) on response functions for the considered properties was

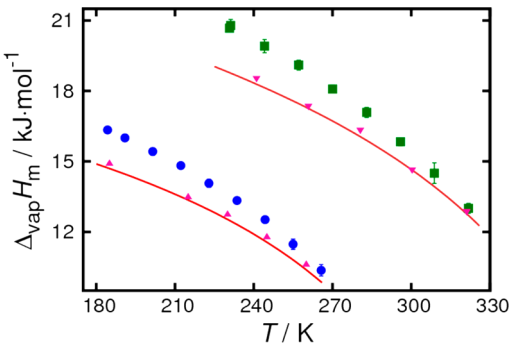

Figure 5. Enthalpies of vaporization of alkanes: (●) C_2H_6 simulation, (▲) C_2H_6 results of Chen and Siepmann,[25] (red line) C_2H_6 Bücker and Wagner EOS,[55] (■) C_3H_8 simulation, (▼) C_3H_8 results of Chen and Siepmann,[25] and (purple line) C_3H_8 Lemmon et al. EOS.[56]

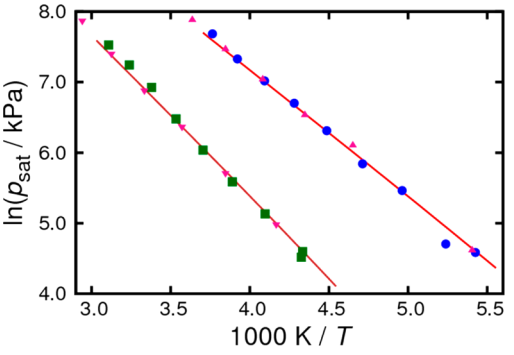

Figure 6. Saturated vapor pressure of alkanes: (●) C_2H_6 simulation, (▲) C_2H_6 results of Chen and Siepmann,[25] (red line) C_2H_6 Bücker and Wagner EOS,[55] (■) C_3H_8 simulation, (▼) C_3H_8 results of Chen and Siepmann,[25] and (purple line) C_3H_8 Lemmon et al. EOS.[56] Estimated uncertainties on simulation are too small to be visible on this scale.

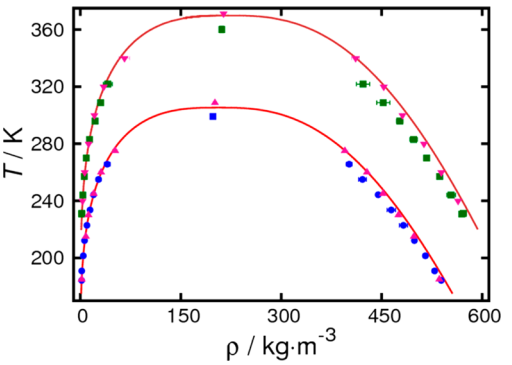

Figure 7. Saturated densities of alkanes: (●) C_2H_6 simulation, (▲) C_2H_6 results of Chen and Siepmann,[25] (red line) C_2H_6 Bücker and Wagner EOS,[55] (■) C_3H_8 simulation, (▼) C_3H_8 results of Chen and Siepmann,[25] and (purple line) C_3H_8 Lemmon et al. EOS.[56]

analyzed. We evaluated the statistical significance of polynomial terms of the response functions using *t*-statistics (Table 3). As expected, linear terms were generally significant for all the functions. However, the effect of σ_{out} on p_{sat} was observed only for alkenes, and its effect on $\Delta_{vap}H$ was noticeable only for alkenes and fluoropropenes. The influence of nonlinear (quadratic) terms appears much sparser across compound classes and properties. For p_{sat}, only alkanes and fluoroalkanes exhibit significance beyond a 50% threshold for quadratic

dx.doi.org/10.1021/jp309119h | J. Phys. Chem. B XXXX, XXX, XXX−XXX

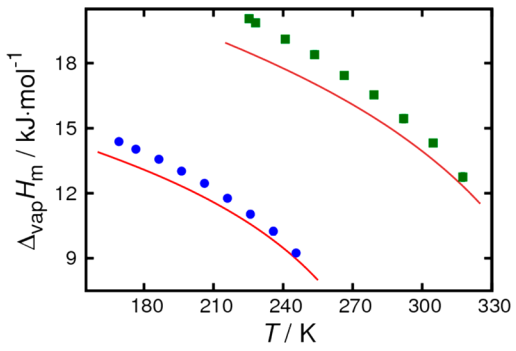

Figure 8. Enthalpies of vaporization of alkenes: (●) C_2H_4 simulation, (red line) C_2H_4 Smukala et al. EOS,[57] (■) C_3H_6 simulation, and (purple line) C_3H_6 Lemmon et al. EOS.[58]

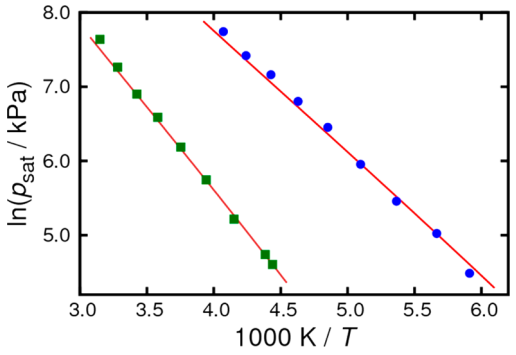

Figure 9. Saturated vapor pressure of alkenes: (●) C_2H_4 simulation, (red line) C_2H_4 Smukala et al. EOS,[57] (■) C_3H_6 simulation, and (purple line) C_3H_6 Lemmon et al. EOS.[58] Estimated uncertainties on simulation are too small to be visible on this scale.

terms, and only two of them, ε_{out}^2 and $\varepsilon_{in}\varepsilon_{out}$, are involved. The same terms appear significant for saturated liquid densities of alkanes, with addition of $\sigma_{in}\varepsilon_{out}$ term. Quadratic terms involving only σ are of significance for densities of alkenes, σ_{in}^2 and $\sigma_{in}\sigma_{out}$. Densities of fluoropropenes have no quadratic terms of significance beyond the 50% threshold. The $\Delta_{vap}H$ functions have significant quadratic terms only for alkanes and alkenes. For alkanes, only the ε_{out}^2 term played a role.

Thermodynamic Properties at p_{sat} = 100 kPa. The calculated VLE curves for the studied compounds are presented in Figures 2−13. The calculated properties at their boiling temperatures at p_{sat} = 100 kPa are presented in Table 1. The agreement between the calculated and experimental T_b and ρ_l values is very good. The enthalpies of vaporization, however, are overestimated for all the studied compounds except fluoroalkanes. It was possible to achieve a much better agreement for enthalpies of vaporization, but in this case saturated vapor pressures became too high. At the same time, exclusion of $\Delta_{vap}H$ from the optimization scheme had a minor effect on the obtained parameters. Therefore, since the obtained Lennard-Jones parameters were optimal for the particular atomic charges used, further improvement of the force field may be possible if a different charge distribution scheme is used.

Vapor−Liquid Coexistence. Enthalpies of vaporization, saturated vapor pressures, and saturated densities are presented in Figures 2−13. Comparison against reference equations of state developed by fitting all available data for the properties within the scope[11,55−60] (as implemented in REFPROP[54]) shows generally good agreement over the entire temperature range. The largest deviations are observed generally between recommended and predicted enthalpies of vaporization. As previously discussed, this agreement could be improved via reweighting of the objective function at the expense of saturated vapor pressure.

Critical Parameters. Critical parameters were obtained via extrapolation with eqs 3 and 4. The calculated values of critical parameters for the considered compounds are compared with the recommended values in Table 2. The calculated T_c agrees with the recommended values within ±10 K, which is a comparable to the performance of group-contribution predictive methods. The critical densities do not deviate from the experimental values by more than ±4.5%. This deviation is somewhat larger than the experimental uncertainty, but still very good in comparison with currently used empirical predictive methods. The largest deviation in p_c is observed for 2,3,3,3-tetrafluoropropene and ethylene, while for the other compounds the agreement is better.

Comparison against previously developed force fields[25,26,28,32] is provided in the figures where possible. The force fields underlying these comparisons were optimized toward the particular classes of compounds represented in each figure. The present results are generally on par with the comparison sets despite the breadth of the optimization behind this work. Predictions of TraPPE-EH[25] for alkanes are generally more accurate than the present model; however, the larger parameter set underlying their fit makes this unsurprising.

As mentioned previously, Raabe and Maginn[32] recently presented an AMBER[64]-based force field parametrized specifically for fluoropropenes. Their force field includes six atom types with the Lennard-Jones parameters fitted to reproduce the heat of vaporization of C_2F_4 and vapor pressures and liquid densities of HFO-1234yf and 3,3,3-trifluoropropene.

Table 1. Comparison of Equation of State[a] and Simulation Values for Molar Enthalpy of Vaporization, $\Delta_{vap}H_m$, and Liquid Density, ρ_l, at Boiling Temperature (p_{sat} = 100 kPa), T_b, for the Compounds Studied

compd	$T_{b,eos}$/K	$\Delta_{vap}H_{m,eos}$/kJ·mol^{-1}	$\rho_{l,eos}$/kg·m^{-3}	$T_{b,calc}$/K	$\Delta_{vap}H_{m,calc}$/kJ·mol^{-1}	$\rho_{l,calc}$/kg·m^{-3}
ethane	184.32 ± 0.09	14.73 ± 0.74	544.1 ± 1.8	186.3 ± 3.1	16.23 ± 0.10	535.9 ± 1.7
propane	230.74 ± 0.29	18.78 ± 0.02	581.2 ± 0.4	232.3 ± 1.7	20.62 ± 0.10	568.5 ± 3.2
ethylene	169.16 ± 0.02	13.54 ± 0.04	568.0 ± 0.4	170.2 ± 1.0	14.31 ± 0.07	564.8 ± 2.7
propene	225.24 ± 0.28	18.48 ± 0.26	610.4 ± 1.7	225.9 ± 1.4	19.98 ± 0.18	601.8 ± 3.1
hexafluoroethane	194.81 ± 0.15	16.16 ± 0.10	1606 ± 22	194.8 ± 2.4	16.27 ± 0.12	1577.2 ± 4.8
octafluoropropane	236.07 ± 0.37	19.79 ± 0.25	1612.7 ± 3.3	237.4 ± 1.1	20.42 ± 0.12	1594.4 ± 3.4
2,3,3,3-tetrafluoropropene	243.37 ± 0.05	20.57 ± 0.23	1263.9 ± 4.4	246.1 ± 1.7	21.99 ± 0.17	1240.7 ± 1.6
(*E*)-1,3,3,3-tetrafluoropropene	253.89 ± 0.33	22.31 ± 0.89	1294.3 ± 4.8	253.9 ± 0.9	23.38 ± 0.28	1265.0 ± 5.1

[a]REFPROP[54] evaluated values, uncertainties are calculated with TDE.[65] Both evaluation methods are consistent to within presented uncertainties.

dx.doi.org/10.1021/jp309119h | J. Phys. Chem. B XXXX, XXX, XXX−XXX

Table 2. Comparison of Equation of State[a] and Simulation Values for Critical Temperature, T_c, Critical Pressure, P_c, and Critical Density, ρ_c, for Compounds Studied

compd	$T_{c,eos}$/K	$p_{c,eos}$/kPa	$\rho_{c,eos}$/kg·m^{-3}	$T_{c,calc}$/K	$p_{c,calc}$/kPa	$\rho_{c,calc}$/kg·m^{-3}
ethane	305.32 ± 0.03	4872 ± 25	206.1 ± 1.3	299.1 ± 0.8	4552 ± 936	198.0 ± 1.6
propane	369.89 ± 0.14	4251 ± 22	220.4 ± 4.3	360.1 ± 2.3	4243 ± 339	211.2 ± 2.0
ethylene	282.35 ± 0.02	5042 ± 7	214.18 ± 0.02	278.5 ± 1.0	5468 ± 405	211.6 ± 1.4
propene	364.21 ± 0.26	4555 ± 76	229.6 ± 3.5	358.1 ± 1.6	4552 ± 318	221.9 ± 2.4
hexafluoroethane	293.03 ± 0.20	3048 ± 26	613 ± 11	299.6 ± 2.4	3275 ± 570	588.0 ± 7.6
octafluoropropane	345.02 ± 0.08	2640 ± 35	627.8 ± 3.5	350.9 ± 1.9	2703 ± 156	613.1 ± 8.6
2,3,3,3-tetrafluoropropene	367.85 ± 0.10	3382 ± 5	475.4 ± 1.0	369.3 ± 1.3	3753 ± 292	459.5 ± 3.2
(*E*)-1,3,3,3-tetrafluoropropene	382.52 ± 0.06	3636 ± 42	489.1 ± 8.0	379.7 ± 2.0	3466 ± 129	466.2 ± 3.9

[a]REFPROP[54] evaluated values, uncertainties are calculated with TDE.[65] Both evaluation methods are consistent to within presented uncertainties except T_c = 364.95 ± 0.26 K evaluated with TDE for propene.

Table 3. Statistical Significance of Coefficients of Various Terms in Response Functions According to t-Criterion[a]

compd	σ_{in}	ε_{in}	σ_{out}	ε_{out}	σ_{in} σ_{in}	σ_{in} ε_{in}	σ_{in} σ_{out}	σ_{in} ε_{out}	ε_{in} ε_{in}	ε_{in} σ_{out}	ε_{in} ε_{out}	σ_{out} σ_{out}	σ_{out} ε_{out}	ε_{out} ε_{out}
Saturated Vapor Pressure														
alkanes	+	+	−	+	−	−	−	−	−	−	+	−	−	+
alkenes	+	+	+	+	−	−	−	−	−	−	−	−	−	−
perfluoroalkanes	+	+	−	+	−	−	−	−	−	−	+	−	−	+
fluoropropenes	−	+	−	−	−	−	−	−	−	−	−	−	−	−
Density														
alkanes	+	+	+	+	−	−	−	+	−	−	+	−	−	+
alkenes	+	+	+	+	+	−	+	−	−	−	−	−	−	−
perfluoroalkanes	+	+	−	+	−	−	−	−	−	−	+	−	−	−
fluoropropenes	+	+	+	+	−	−	−	−	−	−	−	−	−	−
Enthalpy of Vaporization														
alkanes	+	+	−	+	−	−	−	−	−	−	−	−	−	+
alkenes	+	+	+	+	+	−	+	−	−	−	−	+	+	−
perfluoroalkanes	+	+	−	+	−	−	−	−	−	−	−	−	−	−
fluoropropenes	+	+	+	+	−	−	−	−	−	−	−	−	−	−

[a]+ means that the coefficient was statistically significant in >50% response functions.

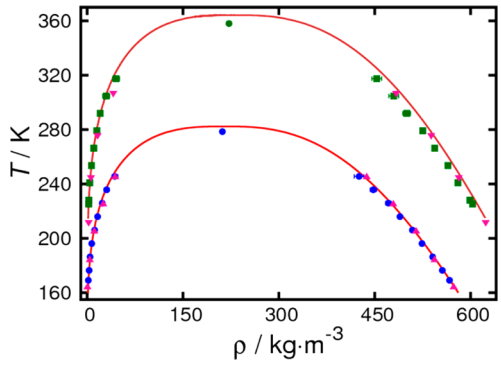

Figure 10. Saturated densities of alkenes: (●) C_2H_4 simulation, (▲) C_2H_4 results of Wick et al.,[26] (red line) C_2H_4 Smukala et al. EOS,[57] (■) C_3H_6 simulation, (▼) C_3H_6 results of Wick et al.,[26] and (purple line) C_3H_6 Lemmon et al. EOS.[58]

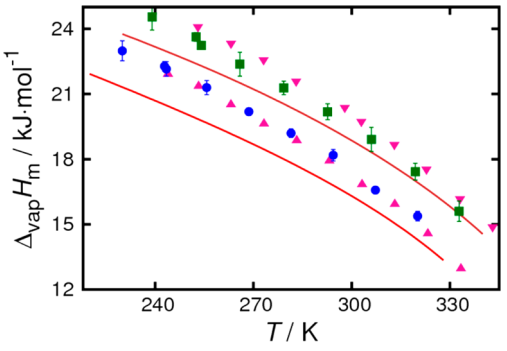

Figure 11. Enthalpies of vaporization of fluoroalkenes: (●) CF_3CFCH_2 simulation, (▲) CF_3CFCH_2 results of Raabe and Maginn,[32] (red line) CF_3CFCH_2 Richter et al. EOS,[11] (■) (*E*)-CF_3CHCHF simulation, (▼) (*E*)-CF_3CHCHF results of Raabe,[35] and (purple line) (*E*)-CF_3CHCHF Lemmon EOS.[60]

While parameters for the atom types of Raabe and Maginn cannot be compared with ours directly, some qualitative differences are apparent. For example, the well depth for hydrogens obtained in this work is about a factor of 2 larger than the corresponding value of Raabe and Maginn. Similar differences are observed between the original AMBER and OPLS-AA assignments. The VLE results reported by Raabe and Maginn for HFO-1234yf[32] and HFO-1234ze(E)[35] are also presented in Figures 11−13. Overall, both force fields perform on a similar level for these two compounds, with the results of Raabe and Maginn showing somewhat better performance for saturated densities (Figure 13). On the other hand, by design, the force field presented here has broader scope as it was also adjusted against the data for alkanes and perfluoroalkanes.

SUMMARY

A systematic, formal procedure for the optimization of molecular force field parameters has been proposed and implemented for prediction of VLE properties of alkanes, alkenes, and their fluorinated derivatives. The Lennard-Jones parameters for 8 atom types (total of 16 parameters) were

dx.doi.org/10.1021/jp309119h | J. Phys. Chem. B XXXX, XXX, XXX−XXX

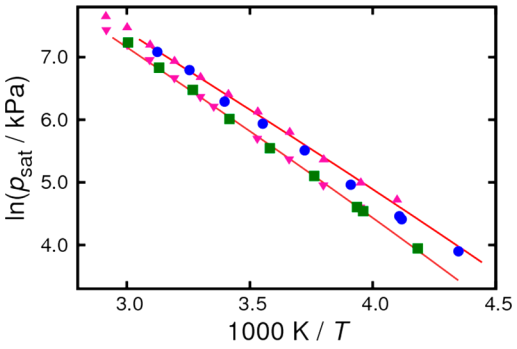

Figure 12. Saturated vapor pressure of fluoroalkenes: (●) CF_3CFCH_2 simulation, (▲) CF_3CFCH_2 results of Raabe and Maginn,[32] (red line) CF_3CFCH_2 Richter et al. EOS,[11] (■) (*E*)-CF_3CHCHF simulation, (▼) (*E*)-CF_3CHCHF results of Raabe,[35] and (purple line) (*E*)-CF_3CHCHF Lemmon EOS.[60] Estimated uncertainties on current simulations are too small to be visible on this scale.

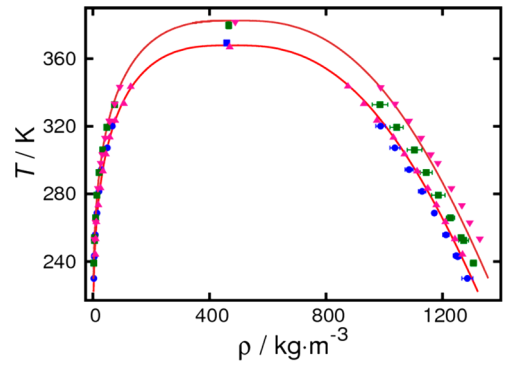

Figure 13. Saturated densities of fluoroalkenes: (●) CF_3CFCH_2 simulation, (▲) CF_3CFCH_2 results of Raabe and Maginn,[32] (red line) CF_3CFCH_2 Richter et al. EOS,[11] (■) (*E*)-CF_3CHCHF simulation, (▼) (*E*)-CF_3CFCH_2 results of Raabe,[35] and (purple line) (*E*)-CF_3CHCHF Lemmon EOS.[60]

optimized to reproduce the enthalpies of vaporization, saturated vapor pressures, and saturated liquid densities derived from the evaluated experimental data. The procedure is based on a solution mapping methodology and includes a modification to central composite design to reduce the necessary simulation set to reasonable scaling. The results of the Monte Carlo molecular simulations utilizing the generated parameters agree well with associated reference equations of state. The formal nature of the proposed approach opens possibilities of automated generation of force field parameters in the future. Further improvements (e.g., selection of the optimal level of theory used for atomic charge assignments) will be possible with the application of additional computational resources.

■ ASSOCIATED CONTENT

Supporting Information

All force field parameters used in this work are available, including the charge distributions for each individual molecule. Note that these charge distributions are not intended to be transferrable. Also included is the full author list for Frisch et al.[41] and Frenkel et al.[65] This material is available free of charge via the Internet at http://pubs.acs.org.

■ AUTHOR INFORMATION

Corresponding Author

*E-mail: kenneth.kroenlein@nist.gov.

Present Address

[§]Guest researcher at the US National Institute of Standards and Technology.

Notes

Trade names are provided only to specify procedures adequately and do not imply endorsement by the National Institute of Standards and Technology. Similar products by other manufacturers may be found to work as well or better. The authors declare no competing financial interest.

■ ACKNOWLEDGMENTS

This study utilized the high-performance computational capabilities of the Biowulf Linux cluster at the National Institutes of Health, Bethesda, MD (http://biowulf.nih.gov) and of the Raritan Linux cluster at the National Institute of Standards and Technology, Gaithersburg, MD.

■ REFERENCES

(1) Maginn, E. J. From Discovery to Data: What Must Happen for Molecular Simulation to Become a Mainstream Chemical Engineering Tool. *AIChE J.* **2009**, *55* (6), 1304−1310.

(2) Rai, N.; Maginn, E. J. Vapor-Liquid Coexistence and Critical Behavior of Ionic Liquids via Molecular Simulations. *J. Phys. Chem. Lett.* **2011**, *2*, 1439−1443.

(3) *Honeywell's low-global-warming-potential refrigerant endorsed by SAE international cooperative research project*; Honeywell: Morris Township, NJ, Dec. 8, 2008.

(4) Honeywell Low Global Warming Technologies. Honeywell. http://www51.honeywell.com/sm/lgwp-uk/applications.html (accessed Aug 15, 2012).

(5) Di Nicola, G.; Polonara, F.; Santori, G. Saturated Pressure Measurements of 2,3,3,3-Tetrafluoroprop-1-ene (HFO-1234yf). *J. Chem. Eng. Data* **2010**, *55*, 201−204.

(6) Kano, Y.; Kayukawa, Y.; Fujii, K.; Sato, H. Ideal-Gas Heat Capacity for 2,3,3,3-Tetrafluoropropene (HFO-1234yf) Determined from Speed-of-Sound Measurements. *Int. J. Thermophys.* **2010**, *31*, 2051−2058.

(7) Tanaka, K.; Higashi, Y.; Akasaka, R. Measurements of the Isobaric Specific Heat Capacity and Density for HFO-1234yf in the Liquid State. *J. Chem. Eng. Data* **2010**, *55*, 901−903.

(8) Di Nicola, C.; Di Nicola, G.; Pacetti, M.; Polonara, F.; Santori, G. P−V−T Behavior of 2,3,3,3-Tetrafluoroprop-1-ene (HFO-1234yf) in the Vapor Phase from (243 to 373) K. *J. Chem. Eng. Data* **2010**, *55*, 3302−3306.

(9) Tanaka, K.; Higashi, Y. Thermodynamic properties of HFO-1234yf (2,3,3,3-tetrafluoropropene). *Int. J. Refrig.* **2010**, *33*, 474−479.

(10) Fedele, L.; Bobbo, S.; Groppo, F.; Brown, J. S.; Zilio, C. Saturated Pressure Measurements of 2,3,3,3-Tetrafluoroprop-1-ene (R1234yf) for Reduced Temperatures Ranging from 0.67 to 0.93. *J. Chem. Eng. Data* **2011**, *56*, 2608−2612.

(11) Richter, M.; McLinden, M. O.; Lemmon, E. W. Thermodynamic Properties of 2,3,3,3-Tetrafluoroprop-1-ene (R1234yf): Vapor Pressure and *p-ρ-T* Measurements and an Equation of State. *J. Chem. Eng. Data* **2011**, *56*, 3254−3264.

(12) Higashi, Y.; Tanaka, K.; Ichikawa, T. Critical Parameters and Saturated Densities in the Critical Region for *trans*-1,3,3,3-tetrafluoropropene (HFO-1234ze(E)). *J. Chem. Eng. Data* **2010**, *55*, 1594−1597.

(13) Tanaka, K.; Takahashi, G.; Higashi, Y. Measurements of the Vapor Pressures and *pρT* properties for *trans*-1,3,3,3-tetrafluoropropene (HFO-1234ze(E)) in the Liquid Phase. *J. Chem. Eng. Data* **2010**, *55*, 2169−2172.

(14) Tanaka, K.; Takahashi, G.; Higashi, Y. Measurements of the Isobaric Specific Heat Capacity for *trans*-1,3,3,3-tetrafluoropropene (HFO-1234ze(E)) in the Liquid Phase. *J. Chem. Eng. Data* **2010**, *55*, 2267−2270.
(15) Tanaka, K.; Higashi, Y. $P\rho T$ Property Measurements for *trans*-1,3,3,3-Tetrafluoropropene (HFO-1234ze(E)) in the Gaseous Phase. *J. Chem. Eng. Data* **2010**, *55*, 5164−5168.
(16) Yamaya, K.; Matsuguchi, A.; Kagawa, N.; Koyama, S. Isochoric Specific Heat Capacity of *trans*-1,3,3,3-Tetrafluoropropene (HFO-1234ze(E)) and the HFO-1234ze(E) + CO_2 Mixture in the Liquid Phase. *J. Chem. Eng. Data* **2011**, *56*, 1535−1539.
(17) Lago, S.; Albo, P. A. G.; Brignolo, S. Speed of Sound Results in 2,3,3,3-Tetrafluoropropene (R-1234yf) and *trans*-1,3,3,3-Tetrafluoropropene (R-1234ze(E)) in the Temperature Range of (260 to 360) K. *J. Chem. Eng. Data* **2011**, *56*, 161−163.
(18) Kagawa, N.; Matsuguchi, A.; Watanabe, K. Measurement of Isobaric Heat Capacity of Gaseous Trans-1,3,3,3-tetrafluoropropene (HFO 1234ze (E)). *Trans. JSRAE* **2011**, *28*, 71−76.
(19) Hulse, R.; Singh, R.; Pham, H. Physical Properties of HFO-1234yf. *3rd International Institute of Refrigeration Conference on Thermophysical Properties and Transfer Processes of Refrigerants,* Boulder, CO, 2009.
(20) Fedele, L.; Brown, J. S.; Colla, L.; Ferron, A.; Bobbo, S.; Zilio, C. Compressed Liquid Density Measurements for 2,3,3,3-Tetrafluoroprop-1-ene (R1234yf). *J. Chem. Eng. Data* **2012**, *57*, 482−489.
(21) Perkins, R. A.; Huber, M. L. Measurement and Correlation of the Thermal Conductivity of 2,3,3,3-Tetrafluoroprop-1-ene (R1234yf) and *trans*-1,3,3,3-Tetrafluoropropene (R1234ze(E)). *J. Chem. Eng. Data* **2011**, *56*, 4868−4874.
(22) Grebenkov, A. J.; Hulse, R.; Pham, H.; Singh, R. Physical Properties and Equation of State for *trans*-1,3,3,3-tetrafluoropropene. *3rd International Institute of Refrigeration Conference on Thermophysical Properties and Transfer Processes of Refrigerants,* Boulder, CO, 2009.
(23) Dong, X.; Gong, M.; Shen, J.; Wu, J. Vapor Liquid Equilibria of the *trans*-1,3,3,3-Tetrafluoropropene (R1234ze(E)) + Isobutane (R600a) System at Various Temperatures from (258.150 to 288.150) K. *J. Chem. Eng. Data* **2012**, *57*, 541−544.
(24) Martin, M. G.; Siepmann, J. I. Transferable Potentials for Phase Equilibria. 1. United-Atom Description of *n*-Alkanes. *J. Phys Chem. B* **1998**, *102*, 2569−2577.
(25) Chen, B.; Siepmann, J. I. Transferable potentials for phase equilibria. 3. Explicit-hydrogen description of normal alkanes. *J. Phys. Chem. B* **1999**, *103*, 5370−5379.
(26) Wick, C. D.; Martin, M. G.; Siepmann, J. I. Transferable potentials for phase equilibria. 4. United-atom description of linear and branched alkenes and alkylbenzenes. *J. Phys. Chem. B* **2000**, *104*, 8008−8016.
(27) Nath, S. K.; Banaszak, B. J.; de Pablo, J. J. A new united atom force field for *alpha*-olefins. *J. Chem. Phys.* **2001**, *114* (8), 3612−3616.
(28) Watkins, E. K.; Jorgensen, W. L. Perfluoroalkanes: Conformational Analysis and Liquid-State Properties from ab Initio and Monte Carlo Calculations. *J. Phys. Chem. A* **2001**, *105*, 4118−4125.
(29) Zhang, L.; Siepmann, J. I. Pressure Dependence of the Vapor-Liquid-Liquid Phase Behavior in Ternary Mixtures Consisting of *n*-Alkanes, *n*-Perfluoroalkanes, and Carbon Dioxide. *J. Phys. Chem. B* **2005**, *109*, 2911−2919.
(30) Hülsmann, M.; Müller, T. J.; Ködderman, T.; Reith, D. Automated force field optimization of small molecules using a gradient-based workflow package. *Mol. Simul.* **2010**, *36* (14), 1182−1196.
(31) Ucyigitler, S.; Camurdan, M. C.; Elliott, J. R. Optimization of Transferable Site-Site Potentials Using a Combination of Stochastic and Gradient Search Algorithms. *Ind. Eng. Chem. Res.* **2012**, *51*, 6219−6231.
(32) Raabe, G.; Maginn, E. J. A Force Field for 3,3,3-Fluoro-1-propenes, Including HFO-1234yf. *J. Phys. Chem. B* **2010**, *114*, 10133−10142.
(33) Paulechka, E.; Kazakov, A.; Frenkel, M. Monte Carlo Simulation of Vapor-Liquid Equilibria for Perfluoropropane (R-218) and 2,3,3,3-Tetrafluoropropene (R-1234yf). *Int. J. Thermophys.* **2010**, *31*, 462−474.
(34) Raabe, G.; Maginn, E. J. Molecular Modeling of the Vapor-Liquid Equilibrium Properties of the Alternative Refrigerant 2,3,3,3-Tetrafluoro-1-propene (HFO-1234yf). *J. Phys. Chem. Lett.* **2010**, *1*, 93−96.
(35) Raabe, G. Molecular Modeling of Fluoropropene Refrigerants. *J. Phys. Chem. B* **2012**, *116*, 5744−5751.
(36) Jorgensen, W. L. Personal communication; Department of Chemistry, Yale University, 2009.
(37) Martin, M. G.; Siepmann, J. I. Novel configurational-bias Monte Carlo method for branched molecules. Transferable potentials for phase equilibria. 2. United-atom description of branched alkanes. *J. Phys. Chem. B* **1999**, *103*, 4508−4517.
(38) Brent, R. P. Some long-period random number generators. *ANZIAM J.* **2007**, *48*, C188−C202.
(39) James, F. RANLUX: A Fortran implementation of the high-quality pseudorandom number generator of Lüscher. *Comput. Phys. Commun.* **1994**, *79* (1), 111−114.
(40) Breneman, C. M.; Wiberg, K. B. Determining atom-centered monopoles from molecular electrostatic potentials. The need for high sampling density in formamide conformational analysis. *J. Comput. Chem.* **1990**, *11*, 361−373.
(41) Frisch, M. J.; Trucks, G. W.; Schlegel, H. B.; Scuseria, G. E.; Robb, M. A.; Cheeseman, J. R.; Montgomery, J. A. J.; Vreven, T.; Kudin, K. N.; Burant, J. C.; et al. *Gaussian 03, Revision D.01*; Gaussian, Inc.: Wallingford, CT, 2004.
(42) Mulliken, R. S. Electronic Population Analysis on LCAO-MO Molecular Wave Functions. I. *J. Chem. Phys.* **1955**, *23* (10), 1833−1831.
(43) Panagiotopoulos, A. Z. Direct determination of phase coexistence properties of fluids by Monte Carlo simulation in a new ensemble. *Mol. Phys.* **1987**, *61*, 813−826.
(44) Panagiotopoulos, A. Z.; Quirke, N.; Stapleton, M.; Tildesley, D. J. Phase equilibria by simulation in the Gibbs ensemble. Alternative derivation, generalization and application to mixture and membrane equilibria. *Mol. Phys.* **1988**, *63*, 527−545.
(45) Smit, B.; De Smedt, P.; Frenkel, D. Computer simulations in Gibbs ensemble. *Mol. Phys.* **1989**, *68*, 931−950.
(46) Allen, M. P.; Tildesley, D. J. *Computer Simulation of Liquids*; Clarendon Press: Oxford, UK, 1987.
(47) Ewald, P. P. Die Berechnung optischer und elektrostatischer Gitterpotentiale. *Ann. Phys.* **1921**, *369*, 253−287.
(48) Martin, M. G.; Frischknecht, A. L. Using arbitrary trial distributions to improve intramolecular sampling in configurational-bias Monte-Carlo. *Mol. Phys.* **2006**, *104*, 2439−2456.
(49) Chen, B.; Siepmann, J. I. Improving the efficiency of the aggregation-volume-bias Monte Carlo algorithm. *J. Phys. Chem. B* **2001**, *105*, 11275−11282.
(50) Frenklach, M. Modeling. In *Combustion Chemistry*; Gardiner, Jr., W. C., Ed.; Springer-Verlag: New York, 1984; Chapter 7, pp 423−453.
(51) Frenklach, M.; Wang, H.; Rabinowitz, M. J. Optimization and analysis of large chemical kinetic mechanisms using solution mapping method—combustion of methane. *Prog. Energy Combust. Sci.* **1992**, *18*, 47−73.
(52) Frenklach, M.; Packard, A.; Feely, R. Optimization of Reaction Models with Solution Mapping. In *Comprehensive Chemical Kinetics*; Carr, R. W., Ed.; Elsevier: New York, 2007; Chapter 6, Vol. *42*, pp 243−291.
(53) Montgomery, D. C. *Design and Analysis of Experiments*; John Wiley & Sons Inc.: New York, 2004.
(54) Lemmon, E. W.; Huber, M. L.; McLinden, M. O. *NIST Standard Reference Database 23: Reference Fluid Thermodynamic and Transport Properties-REFPROP, Version 9.0*; National Institute of Standards and Technology, Standard Reference Data Program: Gaithersburg, MD, 2010.
(55) Bücker, D.; Wagner, W. A Reference Equation of State for the Thermodynamic Properties of Ethane for Temperatures from the

Melting Line to 675 K and Pressures up to 900 MPa. *J. Phys. Chem. Ref. Data* **2006**, *35* (1), 205−266.
(56) Lemmon, E. W.; McLinden, M. O.; Wagner, W. Thermodynamic Properties of Propane. III. A Reference Equation of State for Temperatures from the Melting Line to 650 K and Pressures up to 1000 MPa. *J. Chem. Eng. Data* **2009**, *54*, 3141−3180.
(57) Smukala, J.; Span, R.; Wagner, W. A New Equation of State for Ethylene Covering the Fluid Region for Temperatures from the Melting Line to 450 K at Pressures up to 300 MPa. *J. Phys. Chem. Ref. Data* **2000**, *29* (5), 1053−1122.
(58) Lemmon, E. W. Personal communication; Thermophysical Properties Division, National Institute of Standards and Technology, 2010.
(59) Lemmon, E. W.; Span, R. Short Fundamental Equations of State for 20 Industrial Fluids. *J. Chem. Eng. Data* **2006**, *51*, 785−850.
(60) Lemmon, E. W. Personal communication; Thermophysical Properties Division, National Institute of Standards and Technology, 2010.
(61) Ruff, O.; Bretschneider, O. Die Bildung von Hexafluoräthan und Tetrafluoräthylen aus Tetrafluorkohlenstoff. *Z. Anorg. Allg. Chem.* **1933**, *210*, 173−183.
(62) Renfrew, M. M.; Lewis, E. E. Polytetrafluoroethylene: Heat-resistant, Chemically Inert Plastic. *Ind. Eng. Chem.* **1946**, *38*, 870−877.
(63) Zernov, V. S.; Kogan, V. B.; Lyubetskii, S. G.; Duntov, F. I. Liquid-vapor equilibrium in the system ethylene + trifluoropropylene. *J. Appl. Chem. USSR* **1971**, *44*, 693−696.
(64) Cornell, W. D.; Cieplak, P.; Bayly, C. I.; Gould, I. R.; Merz, K. M., Jr.; Ferguson, D. M.; Spellmeyer, D. C.; Fox, T.; Caldwell, J. W.; Kollman, P. A. A Second Generation Force Field for the Simulation of Proteins, Nucleic Acids, and Organic Molecules. *J. Am. Chem. Soc.* **1995**, *117*, 5179−5197.
(65) Frenkel, M.; Chirico, R. D.; Diky, V.; Muzny, C. D.; Kazakov, A. F.; Magee, J. W.; Abdulagatov, I. M.; Kroenlein, K.; Diaz-Tovar, C. A.; Kang, J. W.; et al. *ThermoData Engine (TDE) Version 7.0 (Pure compounds, Binary Mixtures, Ternary Mixtures, and Chemical Reactions)*; NIST Standard Reference Database 103b; Standard Reference Data Program; National Institute of Standards and Technology: Gaithersburg, MD, 2012.